T-TST-REG-03-2023-00032

Monitoring the Terahertz Response of Skin Beneath Transdermal Drug Delivery Patches Using Sparse Deconvolution

Xavier E. Ramirez Barker, Gonçalo Costa, Rayko I. Stantchev, Arturo I. Hernandez-Serrano, Gabit Nurumbetov, David M. Haddleton and Emma Pickwell-MacPherson, *Senior member, IEEE*

***Abstract*—Terahertz (THz) spectroscopy is a technique proving extremely useful for investigating various biomedical applications by virtue of its high sensitivity in the measurement of water content and non-ionizing nature. By combining this with sparse deconvolution, the THz response of skin directly underneath transdermal drug delivery (TDD) patches was isolated and reconstructed to determine the skin water content *in vivo*. Verification for this method was given by a comparison of skin measured through patches using sparse deconvolution, and skin measurements immediately following patch removal processed with standard approaches. It was found that patches with a non-permeable film backing hydrated the skin to a greater extent than permeable woven polyester fiber backed patches and that this hydration effect primarily occurs within the first 30 minutes of patch application and lasts for at least 24 hours given that the patch remains applied. We demonstrate the effectiveness of this sparse reconstruction method to track hydration levels through layers such as patches and identify scope for further applications including TDD patch development and wound healing techniques and monitoring.**

***Index Terms*—Skin hydration, sparse deconvolution, terahertz imaging, transdermal drug delivery.**

I. INTRODUCTION

TERAHERTZ time-domain spectroscopy (THz TDS) has been employed in the study of various biomedical processes. This is primarily due to its strong attenuation by water molecules and non-ionizing nature resulting in an attractive avenue for this research. For example, successful *in vivo* studies have been conducted for evaluating the healing process of human scars [1], assessing corneal hydration levels [2] and early screening of diabetic foot syndrome [3]. This strong attenuation, caused by the high absorption coefficient of water at THz frequencies leads to a high sensitivity of THz light to water content, providing unique information not available via other approaches. Since most polymers and other packaging materials have a low water content, THz light is able to see through them and has demonstrated potential in security applications [4]. Similarly, transdermal drug delivery (TDD) patches are typically made from lightweight fabric/polymer and THz light is able to pass through them with minimal attenuation. In this study, we exploit the sensitivity of THz light to water along with its ability to see through TDD patch materials, to probe skin hydration whilst the patch is still being worn. The high attenuation by the skin requires reflection geometry to be used for such measurements as the penetration depth into living tissues is limited and thus we need to use sparse deconvolution to separate out the reflections from the patch and the skin. A key benefit of the high sensitivity to water is the ability to monitor the occlusion of skin, which is when the natural loss of water through the skin barrier (sweating) has been obstructed leading to a buildup of water in the stratum corneum altering the hydration profile [5]. Additionally, variations in pressure applied to skin can cause a compression of the tissue leading to changes in the water content and the density of biological background hence the THz response is affected [6]. Observation of skin hydration in general has been exploited in the research and development into moist wound healing methods. Dry, moist and wet healing methods were compared and contrasted by Junker *et al* [7]. It was shown that, compared to standard dry healing methods, a controlled wet environment promoted healing and reduced scar formation. Emerging moist healing methods using various commonly available dressings have been shown to effectively utilize the benefits of this healing method [8]. Silicone gel sheeting is used to occlude severely burned skin as a treatment method, due to the increased water content helping with the burn healing process. Wang *et al.* studied the occlusive effects of silicone gel sheets applied to skin using THz measurements [9].

This benefit of high sensitivity to water content is especially relevant to TDD through medical patches, as skin hydration can be closely linked to the efficacy of drug delivery [10]. TDD is being used for an increasing number of applications, varying from localized pain relief [11] to controlling the symptoms of Parkinson's disease [12]. This approach to drug delivery is being used as it can avoid issues with other delivery methods, such as potential side effects from the liver or gastrointestinal tract metabolizing the drug or the use of needle injections.

This paragraph of the first footnote will contain the date on which you submitted your paper for review, which is populated by IEEE. This work was partially funded by the Engineering and Physical Sciences Research Council (EPSRC) (EP/S021442/1 and EP/V047914/1) and the Royal Society Wolfson Merit Award (EPM). The patches used in this study were manufactured and donated free of charge by Medherant Ltd.

Xavier E. Ramirez Barker, Gonçalo Costa, Rayko I. Stantchev, Arturo I. Hernandez-Serrano and Emma Pickwell-MacPherson are with the Department of Physics, University of Warwick, Coventry, CV4 7AL, UK (emails: x.barker@warwick.ac.uk, goncalo.costa@warwick.ac.uk, rayko.stantchev@warwick.ac.uk, arturo.hernandez-serrano@warwick.ac.uk and e.macpherson@warwick.ac.uk). David M. Haddleton is with the Department of Chemistry, University of Warwick, Coventry, CV4 7AL, UK (email: D.M.Haddleton@warwick.ac.uk). Gabit Nurumbetov is with Medherant Ltd, University of Warwick Science Park, Sir William Lyons Road, Coventry CV4 7EZ, UK (email: g.nurumbetov@medherant.co.uk)

D. M. Haddleton is the Chief Scientific Officer of Medherant Ltd and G. Nurumbetov is an employee of Medherant Ltd. The University of Warwick is a minority shareholder of Medherant Ltd.

The data contained within this paper is available at: https://doi.org/10.6084/m9.figshare.23601006.v1 (accessed on 29/06/2023).

Color versions of one or more of the figures in this article are available online at http://ieeexplore.ieee.org.

Additionally, this simple delivery method is easy for care workers to follow, in the case of patients lacking the ability to take treatments themselves. A further benefit is a greater degree of control over the drug release for the whole time period of drug treatment maintaining the requited therapeutic dose [13]. The functionality of TDD patches can be greatly affected by the design of the patch. By changing the backing material of the patch, the occlusive property of the patch can be controlled to some extent. In cases where the drug is potentially toxic to the wrong person which can occur via transfer, for example, a fully occlusive backing material can be used to ensure no leakage of the drug. Furthermore, by preventing any drug leakage the dosage can lead to better control giving a more effective treatment. However, it has been found that highly occlusive backing materials can lead to skin irritation due to the buildup of water [14]. Thus, less occlusive backing materials can be preferable when the drug treatment allows for it. The adhesive material used for the TDD patch can affect how securely the patch will remain in place, the drug load possible and ease of patch removal [15].

The reflected signals off different layers or "echoes" for THz TDS in reflection geometry can partially or totally overlap, especially in the case of TDD patch measurements due to their thin thickness, requiring deconvolution to accurately resolve these overlapping reflections and extract relevant sample information. Crucially, these signals have a sparse representation due to the limited number of echoes containing all the significant information, and so only a limited number of data points have non-zero values when ignoring noise. The sparse constraint can be applied to such signals, allowing sparse deconvolution to be utilized to retrieve the impulse-response function via an inverse problem where detection and estimation of the signal are performed jointly. Sparse deconvolution has been shown to perform extremely well in many areas, from processing seismic data whilst being robust against outliers [16] to improving the resolution of fluorescence microscopy for live-cells [17]. THz TDS sparse deconvolution has met success for the nondestructive evaluation and characterization of a 17th century easel painting [18] and subsurface damage visualization for carbon fiber-reinforced composites [19].

In this paper, a sparse deconvolution method is used to process *in vivo* reflected THz measurements from TDD patches applied to skin, with a view to being able to evaluate the skin hydration through the patches. Other analytical approaches have failed due to the thin TDD patches causing overlapping pulse echoes. The remainder of the paper is organized as follows. In Section II sparse deconvolution for THz TDS is outlined, followed by a method to obtain the reconstructed skin reflection peak-to-peak from the sparse result. Section III introduces the experimental setup and protocol used for *in vivo* measurements taken in both a 2-hour and 24-hour long experiment. The results and discussion for the two experiments are presented in section IV, along with measurements to describe the patches. Finally, the conclusions of this work are contained in section V.

II. Sparse Deconvolution Applied to THz

For reflective THz imaging in time domain, the incident THz pulse *i(t)* is convoluted with the impulse-response function *h(t)* to give the measured THz reflected signal *y(t)*:

$$y(t) = i(t) \otimes h(t) = \int_{-\infty}^{+\infty} i(\tau)h(t-\tau)d\tau. \qquad (1)$$

Sample information, such as the structure and properties, are contained within the impulse-response function. In practice, the discrete version of (1) is experimentally obtained, given by:

$$y_n = \sum_{m=0}^{M-1} i_m h_{n-m} + e_n\,. \qquad (2)$$

Here, $y_n = y(nT_s)$, $i_m = i(mT_s)$, T_s is the sampling period, n and m are the indices of data points, M is the length of the data set and e_n accounts for the noise in the measurement due to the measurement system and materials. By letting column vectors **y**, **i**, **h**, and **e** collect y_n, i_n, h_n and e_n respectively then (2) becomes:

$$\mathbf{y} = \mathbf{A}\mathbf{h} + \mathbf{e}, \qquad (3)$$

where **A** is the square Toeplitz matrix where delayed versions of **i** make up its columns [20]. Each consecutive column has **i** delayed by a further one element, until the whole of **i** has been cycled through and a square matrix has resulted.

The key focus of sparse deconvolution is obtaining the solution for the following l_0 regularized optimization problem, which exploits the sparse constraint by approximating **y** with **Ah**, where **h** crucially is a sparse sequence. Being a sparse sequence demands that **h** only has few non-zero elements. The l_0 regularized optimization problem is defined by:

$$\min_{\mathbf{h}} \frac{1}{2}\|\mathbf{A}\mathbf{h} - \mathbf{y}\|_2^2 + \lambda\|\mathbf{h}\|_0\,, \qquad (4)$$

where $\|\ \|_2$ and $\|\ \|_0$ represents the l_2-norm and l_0-norm respectively. Here, λ is the sparsity factor chosen to select the tradeoff between the sparsity of **h** and the residue norm. The higher this sparsity factor is set, the more sparse the resulting **h** will be, and so the smaller the second term will be. The first term represents the distance between the approximation **Ah** and actual measured reflected THz signal **y**. However, the solution to this problem is known to be non-deterministic polynomial-time hard in general [21] and it has been shown that an approximation using the l_1-norm in place of the l_0-norm performs well whilst guaranteeing a global optimum, unlike when using the l_0-norm [22]. Now, by using the l_1-norm for **h** instead, $\|\mathbf{h}\|_1$, (4) becomes:

$$\min_{\mathbf{h}} \frac{1}{2}\|\mathbf{A}\mathbf{h} - \mathbf{y}\|_2^2 + \lambda\|\mathbf{h}\|_1\,. \qquad (5)$$

To solve (5) an iterative shrinkage algorithm will be

employed, where soft-thresholding is applied to the result of a vector multiplication for each iteration:

$$\mathbf{h}_{i+1} = S_{\lambda\tau}(\mathbf{h}_i - \tau\mathbf{A}^{\mathrm{T}}(\mathbf{A}\mathbf{h}_i - \mathbf{y})), \tag{6}$$

where τ is a suitable step size, constrained by:

$$\tau < \frac{2}{\|\mathbf{A}^{\mathrm{T}}\mathbf{A}\|_2}, \tag{7}$$

in order to ensure convergence. The soft-thresholding component is contained within the operator $S_{\lambda\tau}$:

$$S_{\lambda\tau}(h[n]) = \begin{cases} h[n] + \lambda\tau & h[n] \leq -\lambda\tau \\ 0 & |h[n]| < \lambda\tau \\ h[n] - \lambda\tau & h[n] \geq \lambda\tau \end{cases}. \tag{8}$$

Now that the sparse result contained in **h** has been obtained, this can be used to reconstruct the individual reflections within the reflected signal **y**. Typically, this sparse result consists of separate small clusters of points to represent each reflection contained within the reflected signal. The points corresponding to the reflection of interest can easily be isolated. By aligning and scaling multiple incident THz pulses with the chosen reflection points' temporal locations and amplitudes respectively, a recreation of the reflection of interest can be created. The peak-to-peak of this reflection can then be measured by combining the magnitude of the most positive and most negative points in the reflection.

For the results contained within this paper, the incident THz pulse was obtained via measuring the reflection off an optically thick piece of quartz and multiplying by -1 for phase correction. A sparsity factor λ=3.5 was chosen, as this gave the best results whilst not over-aggressively soft-thresholding for the data sets we were using. A step size $\tau = 1.2/\|\mathbf{A}^{\mathrm{T}}\mathbf{A}\|_2$ was selected as a trade-off between run-time and accuracy whilst abiding by the constraint stated in (7). The iteration outlined in (6) was repeated 2000 times for each result, chosen for the same reasons as the step size.

III. Samples and Experiment

Ethical approval was obtained for this study from the Biomedical Scientific Research Ethics Committee, BSREC, (REGO-2018-2273 AM03). Written informed consent was obtained from each volunteer prior to their involvement in the study. A Menlo Systems Tera K15 fibre-coupled THz TDS system was used for the acquisition of the *in-vivo* skin measurements. The emitter and the detector were arranged on optical rails and mounted below a quartz window, at a 30° angle of incidence to it, as shown in fig. 1. Before volunteer measurements began, a reference measurement was taken by setting a thick piece of quartz at the sample recording position. This was measured each day to account for any daily variations in the THz signal produced by the system. An example of a reference pulse used in this paper is shown in fig. 2. A quartz reflection was used as the reference since a quartz imaging window was used for the measurements taken on volunteers. Further, sparse deconvolution performs best when the reference used closely resembles the shape of sample reflections, thus a quartz reference is the closest reference obtainable. For the sample measurements, the volunteers placed their volar forearm atop of the quartz window for 1 minute to acquire approximately 280 reflected THz pulses from a single point on their skin for each region of interest. To ensure a consistent contact of skin with the quartz imaging window, as to avoid the occurrence of air gaps between the two for example, a pressure sensor was placed on each side of the imaging window and the volunteers kept a consistent pressure in the 1.5 – 2.5 Ncm^{-2} range. This pressure range was found to be comfortable and easy for the volunteers to maintain.

TDD patches with two types of backing materials and with different excipient percentages were placed on both volar forearms of the volunteers, as demonstrated in fig. 3. The patches placed on the left volar forearm were the occlusive poly(ethylene terephthalate) film backed ones, whilst the partially occlusive polyester fiber woven backed patches were placed on the right volar forearm. The excipients in TDD patches, serving as vehicles for the drugs in the patches, boost the latter's drug delivery rate. To analyze if different percentages of these excipients have an effect on the skin's hydration levels, three patches, each with a different excipient concentration (0%, 3% and 6%), were placed on each arm. In addition to the patches, a region of skin on both volar forearms was designated as a control region to be measured and left untreated to account for a person's natural temporal variation of their skin hydration. These 4 regions on each arm constituted the regions of interest to be measured. In this experiment the excipient in use was propylene glycol ($CH_3CH(OH)CH_2OH$) [23] and the aforementioned excipient concentrations were chosen as these are commonly found in commercial TDD patches. It is noteworthy that propylene glycol is reported to dehydrate skin [24], while the act of occluding the skin by wearing a patch will increase the hydration, it is therefore interesting to see the relative effects of the changes in propylene glycol concentration and the type of patch backing material used. The adhesive material used for the patches was a proprietary polyurea cross-linked thermoset, with 10% Transcutol® present [15]. These non-active patches were manufactured by Medherant Ltd. No other drugs were present in the patches to isolate any changes on the skin as a consequence of the patches backing material and excipient. The findings on the effects of the excipients are detailed in [25]. The key extension in this work is that we show that through sparse deconvolution, we can evaluate the skin beneath the patch while the patch is still being worn.

The skin on the volunteer's volar forearm was measured before applying the TDD patches. Once the patches were applied, the imaging window was placed atop of the patches and the skin was measured with the patches on. During each set of measurements, the untreated control region was also measured for both arms. For the 2-hour experiment the measurements were taken with the patches on the volar forearm, i.e. through the patches, at 0 minutes, 30 minutes and 2 hours after the

patches were applied for 8 volunteers. For the 24-hour experiment measurements on 14 volunteers were taken immediately following patch application and then 24 hours later with both the patches still applied and then shortly after removing them. By conducting these two experiments with measurements at various time intervals both the short- and long-term effects on skin of the TDD patches and the excipients contained within them can be examined. As the 24-hour experiment has measurements shortly before patch application and shortly following patch removal, these patchless measurements can be used to verify our sparse reconstruction method applied to the paired patch measurements. Before the start of each measurement the subjects acclimatized for a period of 20 minutes in the controlled environment of the laboratory to exclude any effects that being in different rooms and environments might have on the skin.

Even with this protocol in place, there are many other factors which significantly impact the condition of skin that could not be controlled for during the 24-hour experiment. For example, the volunteer could have gone swimming, showered or significantly changed diet and water consumption between measurements. To account for such variations, the normalized relative change (NRC) [26] was calculated:

$$\mathrm{NRC}(\%) = \frac{(X_{St} - X_{Sb}) - (X_{Ct} - X_{Cb})}{X_{Sb} + (X_{Ct} - X_{Cb})} \times 100\%, \quad (9)$$

where X_{St} is the measured parameter at time t following application of a patch and X_{Sb} is the measured parameter at the same region of skin before the patch was applied. X_{Ct} and X_{Cb} are the same parameters for the control region which did not have a patch applied. $X_{Ct} - X_{Cb}$ represents the variation of the skin between the measurements, which accounts for the other aforementioned variations in the volunteers' skin, such as if the volunteer had showered between the measurements. This processing was not required for the 2-hour experiment as this was over a shorter time period and volunteers remained in controlled room conditions. Additionally, they avoided any factors which could significantly affect the skin, such as applying moisturizer.

IV. Results and Discussion

Firstly, THz reflection data for the patches alone will be presented, as to characterize their THz response and demonstrate the sparse deconvolution results. Both a film and woven patch of 0% excipient were placed directly onto the quartz imaging window and measured using the same system as described in the previous section. Fig. 4a contains the measured THz data, **y**, for a single point scan through the center of the film patch, in reflection geometry. This means that the first reflection corresponds to the quartz-patch interface and the second reflection corresponds to the patch-skin interface. The sparse deconvolution result, **h**, is also shown. Lastly, the results from using a standard THz processing method fully described in [25] are also presented. This processing method includes accounting for the use of a quartz imaging window and the application of a double Gaussian filter centered at 0.6 THz. Fig. 4b shows the same data but for the woven patch. The sparse result tracks the center of the first peak of the THz reflection. A clear difference between the optical thickness of the two patches can be observed, due to the optical delay being much larger between the two surface reflections for the woven patch. For the film patch, there is a clear overlap between its bottom and top surface reflections. This overlap results in interference, destructive for the first reflection but constructive for the second reflection, due to the incident THz pulse shape (as shown in fig. 2) and the resulting phase shift. The sparse deconvolution result is able to account for this overlap and interference, recovering the temporal location and relative amplitude associated with the overlapping reflections. For the purposes of this paper, the sparse reconstruction method presented can recover useful sample information in such overlaps. It can also be noticed that the second reflection from the woven backed patch is significantly smaller than the second reflection from the film patch. As the woven patch is thicker, the reflection has become more attenuated during this increased travel time. Additionally, the woven patches have a refractive index closer to that of skin than the film patches did, thus a relatively smaller reflection from the patch-skin boundary for the woven patches resulted. The refractive index of the patches at 0.6 THz were calculated from transmission measurements to be 1.523 for the woven patches and 1.464 for the film patches. This can be compared to a bare skin refractive index of 1.904, also at 0.6 THz, obtained by standard reflection approaches introduced earlier in this section.

Fig. 5a shows the average NRC, defined in (9), for the peak-to-peak of the reconstructed skin reflection for 14 volunteers. This reconstruction was made using the sparse result of *in vivo* skin measurements with a TDD patch applied, with these measurements containing the reflections highlighted in the schematic shown in fig. 1. Then, following the steps outlined in section II, the reconstruction and the peak-to-peak measurement were obtained. The first data set was taken shortly following patch application and the second 24 hours after application. For both patch types and each excipient percentage, the NRC can be obtained by using the reconstruction from these patch measurements together with the control measurements taken at the same times, following the procedure outlined in section III. Measurements taken with the film and woven backed patches are shown on the left and right sections of the figure respectively, with the color indicating excipient level. The error bars indicate the standard error of the mean.

All results presented in fig. 5a demonstrate a significant decrease in peak-to-peak NRC, which is linked to an increase in hydration level [27]. This signifies that the patches have led to water collecting in the skin beneath them due to the aforementioned occlusion effect. As the decrease in the woven patch data is less severe, it can be determined that these patches are more breathable. This demonstrates the ability of this method to discern the occlusive characteristics of various medical patches and bandages. Furthermore, a slight trend in decreasing magnitude of the peak-to-peak NRC as excipient level increases can be observed, indicating a decrease in skin hydration with higher excipient level. However, this trend is mostly within the errors of each individual result, demonstrating the need for further

measurements to ascertain this relationship. Regardless, this highlights the potential of this method for monitoring the effects of transdermal drugs on skin hydration beneath patches or bandages. The errors for the woven patches are smaller than those for the film patches. As shown earlier in this section, the woven patches were thicker which resulted in a larger optical separation between the quartz-patch and patch-skin reflection. Thus, the sparse deconvolution could perform more accurately and consistently, resulting in a smaller error.

Fig. 5b contains data taken as a verification for our sparse reconstruction method and as a comparison to previous work covered in [25]. The procedure is very similar to that used above, however the measurements were taken shortly before patch application and immediately after the patches were removed after 24 hours of them being applied. This meant that the skin could be directly measured, without the need of any sparse deconvolution and reconstruction to obtain and separate the skin data from under the patch. Therefore, these similar direct skin measurements can be compared to those obtained via our sparse reconstruction method.

By comparing fig. 5a and b it can be seen that a significant reduction in the NRC for the peak-to-peaks are obtained in both data sets, but the measurements taken with the patches remaining applied show a noticeably larger reduction. Furthermore, in the skin only measurements shown in fig. 5b there is no longer a clear significant difference between the patch types. An explanation for both of these differences is the nature of removing the patches before the 24-hour measurements allows some time for the skin to breath and become less hydrated, resulting in a smaller peak-to-peak NRC. Additionally, as the skin under the film patches was initially more hydrated it would dehydrate to a normal state at a faster rate than the skin under the woven patches, proceeding to a less obvious difference between them. This distinction between the types of patches reveals the benefit of monitoring the skin whilst the patch is still applied, which our sparse reconstruction method allows. Furthermore, we expect that the NRC in the peak-to-peak to be more accurate following the sparse method, as the skin hydration can be monitored without patch removal, and consequently without time for the skin to dehydrate.

To demonstrate the correlation between the NRC for the peak-to-peaks contained in fig. 5a and fig. 5b we have plotted them against each other as shown in fig. 6 and calculated the Pearson correlation coefficient from the line of best fit for these results. With the coefficient being 0.97, it demonstrates the strong correlation between the results with the patch on and with only skin, providing evidence to the accuracy of our sparse reconstruction method used for the data with the patch applied.

A further experiment was conducted for investigating the shorter-term response of skin to the patches, collecting data from 8 volunteers. This time, measurements were taken immediately following patch application, 30 minutes after and finally 2 hours after application. All measurements were taken through the patch and reconstructed using our sparse method. Results from these measurements can be seen in fig. 7, where the left section contains the film results and the right contains woven ones. This time, the color of the bars signifies the measurement time following patch application with the excipient level changes for each cluster of bars and is denoted on the x-axis. Unlike in the previous data presented, here we do not use the average NRC in the peak-to-peak, but the average raw peak-to-peak itself. As this experiment was conducted over a shorter time period, only 2 hours, and volunteers remained in consistent laboratory room conditions during which other factors that affect the skin were controlled. The error bars indicate the standard error of the mean.

A clear trend of the measurements taken immediately after patch application being higher than the other two measurements for that patch type and excipient level can be observed in fig. 7. As explained previously, a higher peak-to-peak indicates less hydrated skin comparatively. Thus, in all cases there is a significant increase in hydration after the patch has been applied for 30 minutes. This hydrating effect drops off between the 30 minute and 2-hour measurements, as there is only a small decrease in peak-to-peak which is generally within the error of these results. Therefore, by considering the 24-hour results too, we can conclude that the majority of the hydrating effect of the patches occurs within the first 30 minutes of their application and lasts for at least 24 hours, if the patch remains on the skin. A very big difference between the average peak-to-peak results for the film backed patches and the woven backed patches can be seen. As explored at the beginning of this section, the THz measurements for these patches look very different. Specifically, a larger optical delay and smaller amplitude for the woven patch reflection as compared to the film patch. This smaller reflection amplitude causes the sparse reconstruction for this reflection to also have a lower peak-to-peak. However, this does not signify that the skin under the woven patch is less hydrated than the skin beneath the film patch but highlights that the hydration information is contained within how this amplitude changes over time. By observing how the average peak-to-peak decreases for the woven data sets compared to the film sets, we can see that there is a greater relative decrease in the film data. Thus, these results agree with the film patches being more occlusive and so having a greater hydrating effect, as found in the 24-hour data. In this case there was only slight variation in skin hydration for the different excipient levels, but in situations such as a burn wound healing under a bandage there are significant hydration level changes [28]. A further application of our sparse reconstruction method could be for other situations where monitoring how the hydration level of skin under patches or bandages changes over time, without having to remove them, would be helpful.

V. Conclusion

In this paper, a sparse reconstruction method has been introduced and successfully employed to *in vivo* THz measurements of various TDD patches. Such a method is required in situations where overlap between reflections occurs, as to retrieve accurate sample information. TDD patch measurements are often such a case, by virtue of the patch's thinness. This method was verified by a comparison of sparse reconstruction results with the patch applied to standard measurements in the same locations immediately before or after the patch was applied or removed, respectively. A significant difference in occlusion properties of patches with different backing materials was found, with a film backing proving to be much more occlusive than a woven backing. It was discovered that the majority of the occlusion effects occurred within the first 30 minutes of patch application and persisted for at least

24 hours if the patch remained applied. A slight difference between excipient levels was observed, with hydration decreasing with higher excipient concentration. However, this was generally within error bars and thus further research into this effect is required. Further work could include using this method to observe wound healing beneath casts or bandages, as the healing process is closely linked to skin hydration levels. Additionally, moist and wet healing methods are gaining traction, as it has been shown that wounds can heal better in moist conditions. This sparse reconstruction method of THz TDS data could be applied to help with research into these healing methods by monitoring hydration levels non invasively.

REFERENCES

[1] S. Fan, B. S. Y. Ung, E. P. J. Parrott, V. P. Wallace, and E. Pickwell-MacPherson, "In vivo terahertz reflection imaging of human scars during and after the healing process," *Journal of Biophotonics,* vol. 10, no. 9, pp. 1143-1151, 2017, doi: https://doi.org/10.1002/jbio.201600171.

[2] Z. D. Taylor *et al.*, "THz and mm-Wave Sensing of Corneal Tissue Water Content: Electromagnetic Modeling and Analysis," *IEEE Transactions on Terahertz Science and Technology,* vol. 5, no. 2, pp. 170-183, 2015, doi: 10.1109/TTHZ.2015.2392619.

[3] G. G. Hernandez-Cardoso *et al.*, "Terahertz imaging for early screening of diabetic foot syndrome: A proof of concept," *Scientific Reports,* vol. 7, no. 1, p. 42124, 2017/02/06 2017, doi: 10.1038/srep42124.

[4] H. B. Liu, H. Zhong, N. Karpowicz, Y. Chen, and X. C. Zhang, "Terahertz spectroscopy and imaging for defense and security applications," *Proceedings of the IEEE,* vol. 95, no. 8, pp. 1514-1527, 2007, doi: 10.1109/JPROC.2007.898903.

[5] Q. Sun, E. P. J. Parrott, Y. He, and E. Pickwell-MacPherson, "In vivo THz imaging of human skin: Accounting for occlusion effects," *Journal of Biophotonics,* vol. 11, no. 2, pp. e201700111-e201700111, 2018, doi: 10.1002/jbio.201700111.

[6] T.-W. Chiu, E. P. MacPherson, J. Wang, R. I. Stantchev, Q. Sun, and A. T. Ahuja, "THz in vivo measurements: the effects of pressure on skin reflectivity," *Biomedical Optics Express,* vol. 9, no. 12, pp. 6467-6467, 2018, doi: 10.1364/boe.9.006467.

[7] J. P. E. Junker, R. A. Kamel, E. J. Caterson, and E. Eriksson, "Clinical Impact Upon Wound Healing and Inflammation in Moist, Wet, and Dry Environments," *Advances in Wound Care,* vol. 2, no. 7, pp. 348-356, 2013/09/01 2013, doi: 10.1089/wound.2012.0412.

[8] K. Nuutila and E. Eriksson, "Moist Wound Healing with Commonly Available Dressings," *Advances in Wound Care,* vol. 10, no. 12, pp. 685-698, 2021/12/01 2020, doi: 10.1089/wound.2020.1232.

[9] J. Wang, Q. Sun, R. I. Stantchev, T.-W. Chiu, A. T. Ahuja, and E. Pickwell-MacPherson, "In vivo terahertz imaging to evaluate scar treatment strategies: silicone gel sheeting," *Biomedical Optics Express,* vol. 10, no. 7, pp. 3584-3590, 2019/07/01 2019, doi: 10.1364/BOE.10.003584.

[10] K. S. Ryatt, M. Mobayen, J. M. Stevenson, H. I. Maibach, and R. H. Guy, "Methodology to measure the transient effect of occlusion on skin penetration and stratum corneum hydration in vivo," *British Journal of Dermatology,* https://doi.org/10.1111/j.1365-2133.1988.tb03222.x vol. 119, no. 3, pp. 307-312, 1988/09/01 1988, doi: https://doi.org/10.1111/j.1365-2133.1988.tb03222.x.

[11] P. Arora and B. Mukherjee, "Design, development, physicochemical, and in vitro and in vivo evaluation of transdermal patches containing diclofenac diethylammonium salt," *Journal of Pharmaceutical Sciences,* vol. 91, no. 9, pp. 2076-2089, 2002, doi: 10.1002/jps.10200.

[12] W. H. Poewe *et al.*, "Efficacy of pramipexole and transdermal rotigotine in advanced Parkinson's disease: a double-blind, double-dummy, randomised controlled trial," *The Lancet Neurology,* vol. 6, no. 6, pp. 513-520, 2007.

[13] O. A. Al Hanbali, H. M. S. Khan, M. Sarfraz, M. Arafat, S. Ijaz, and A. Hameed, "Transdermal patches: Design and current approaches to painless drug delivery," *Acta Pharmaceutica,* vol. 69, no. 2, pp. 197-215, 2019, doi: doi:10.2478/acph-2019-0016.

[14] J. F. G. M. Hurkmans, H. E. BoddÉ, L. M. J. Van Driel, H. Van Doorne, and H. E. Junginger, "Skin irritation caused by transdermal drug delivery systems during long-term (5 days) application," *British Journal of Dermatology,* https://doi.org/10.1111/j.1365-2133.1985.tb02321.x vol. 112, no. 4, pp. 461-467, 1985/04/01 1985, doi: https://doi.org/10.1111/j.1365-2133.1985.tb02321.x.

[15] E. L. Tombs, V. Nikolaou, G. Nurumbetov, and D. M. Haddleton, "Transdermal Delivery of Ibuprofen Utilizing a Novel Solvent-Free Pressure-sensitive Adhesive (PSA): TEPI® Technology," *Journal of Pharmaceutical Innovation,* vol. 13, no. 1, pp. 48-57, 2018/03/01 2018, doi: 10.1007/s12247-017-9305-x.

[16] A. Gholami and M. D. Sacchi, "A Fast and Automatic Sparse Deconvolution in the Presence of Outliers," *IEEE Transactions on Geoscience and Remote Sensing,* vol. 50, no. 10, pp. 4105-4116, 2012, doi: 10.1109/TGRS.2012.2189777.

[17] W. Zhao *et al.*, "Sparse deconvolution improves the resolution of live-cell super-resolution fluorescence microscopy," *Nature Biotechnology,* vol. 40, no. 4, pp. 606-617, 2022/04/01 2022, doi: 10.1038/s41587-021-01092-2.

[18] J. Dong, A. Locquet, M. Melis, and D. S. Citrin, "Global mapping of stratigraphy of an old-master painting using sparsity-based terahertz reflectometry," *Scientific Reports,* vol. 7, no. 1, pp. 1-12, 2017, doi: 10.1038/s41598-017-15069-2.

[19] J. Dong *et al.*, "Visualization of subsurface damage in woven carbon fiber-reinforced composites using polarization-sensitive terahertz imaging," *NDT and E International,* vol. 99, no. July, pp. 72-79, 2018, doi: 10.1016/j.ndteint.2018.07.001.

[20] T. Blu, P. L. Dragotti, M. Vetterli, P. Marziliano, and L. Coulot, "Sparse sampling of signal innovations: Theory, algorithms, and performance bounds," *IEEE Signal Processing Magazine,* vol. 25, no. 2, pp. 31-40, 2008, doi: 10.1109/MSP.2007.914998.

[21] B. K. Natarajan, "Sparse Approximate Solutions to Linear Systems," *SIAM Journal on Computing,* vol. 24, no. 2, pp. 227-234, 1995, doi: 10.1137/s0097539792240406.

[22] T. Blumensath and M. E. Davies, "Iterative Thresholding for Sparse Approximations," *Journal of Fourier Analysis and Applications,* vol. 14, no. 5, pp. 629-654, 2008/12/01 2008, doi: 10.1007/s00041-008-9035-z.

[23] V. Carrer *et al.*, "Effect of propylene glycol on the skin penetration of drugs," *Archives of Dermatological Research,* vol. 312, no. 5, pp. 337-352, 2020/07/01 2020, doi: 10.1007/s00403-019-02017-5.

[24] A. Kolesnikov *et al.*, "THz monitoring of the dehydration of biological tissues affected by hyperosmotic agents," *Physics of Wave Phenomena,* vol. 22, pp. 169-176, 07/01 2014, doi: 10.3103/S1541308X14030029.

[25] X. Ding *et al.*, "Quantitative evaluation of transdermal drug delivery patches on human skin with in vivo THz-TDS," *Biomedical Optics Express,* vol. 14, no. 3, pp. 1146-1158, 2023/03/01 2023, doi: 10.1364/BOE.473097.

[26] H. Lindley-Hatcher *et al.*, "A Robust Protocol for In Vivo THz Skin Measurements," *Journal of Infrared, Millimeter, and Terahertz Waves,* vol. 40, 09/01 2019, doi: 10.1007/s10762-019-00619-8.

[27] H. Lindley-Hatcher, A. I. Hernandez-Serrano, J. Wang, J. Cebrian, J. Hardwicke, and E. Pickwell-MacPherson, "Evaluation of in vivo THz sensing for assessing human skin hydration," *Journal of Physics: Photonics,* vol. 3, no. 1, p. 014001, 2020/12/14 2021, doi: 10.1088/2515-7647/abcb71.

[28] A. Terezaki *et al.*, "Ulvan/gelatin-based nanofibrous patches as a promising treatment for burn wounds," *Journal of Drug Delivery Science and Technology,* vol. 74, p. 103535, 2022/08/01/ 2022, doi: https://doi.org/10.1016/j.jddst.2022.103535.

Xavier E. Ramirez Barker received his combined BSc and MSc degree in Physics from the University of Warwick, UK, in 2018. During the MSc, he worked on simulating a magnetic cooling system using the magnetocaloric effect. He is currently working towards a PhD degree at the University of Warwick., focusing on signal processing techniques for THz.

His research interests include sparse deconvolution, finite rate of innovation and THz spectroscopy.

Gonçalo Costa received his BSc degree in Mathematics and Physics from the University of Dundee in 2019, where he worked on the development of an Yb-doped fiber laser, and a MSc degree in Particles, Strings & Cosmology in 2021 from the University of Durham, where he studied Sterile Neutrinos as Dark Matter candidates. He is currently working towards a PhD degree at the University of Warwick under the supervision of Prof. E. Pickwell-MacPherson. His research interests include THz single-pixel imaging and spectroscopy.

Rayko I. Stantchev obtained a BSc degree in Mathematics and Physics combined honors in 2013 at the university of Exeter. Immediately after, without a Master's degree, at Exeter he started a PhD in experimental physics working with a THz spectrometer and spatial light modulators. His PhD focused on the experimental implementation of non-invasive THz imaging using single-element detectors, with the addition of adaptive undersampling techniques.

Upon completion of his thesis, in 2017, he moved to Hong Kong for a postdoc with the THz group of Prof. E. Pickwell-MacPherson in the Chinese university of Hong Kong. In 2021, the THz group in Hong Kong completely moved to the UK at the University of Warwick and Rayko was based here until Aug/2022. Then he moved to Taiwan to be an assistant professor at the National Sun Yat-sen University where he is currently at, whilst holding an honorary research fellow position at the University of Warwick.

Arturo I. Hernandez-Serrano received a BSc degree in Physics with summa cum laude in 2013 at the university of Guanajuato in Mexico working in the development of fiber optics-based devices. Later, a Master and PhD degree in 2014 and 2018, respectively, at the Research center of optics in Mexico working with THz technologies in medical applications and photonics. His PhD thesis is focused in the development of novel photonic devices using 3D printing techniques for the THz band.

Since 2018, he moved to the UK at the University of Warwick working under the supervision of Prof. Emma MacPherson in the development of non-invasive techniques for the treatment of skin diseases using THz spectroscopy.

David M. Haddleton obtained his PhD from the University of York in 1986 and spent time as a PDRA in Toronto before joining ICI PLC. After 6 years in industry, he moved to Warwick in 1993 becoming full Professor in 1998. He has graduated 85 PhD students from Warwick and published over 500 publications. He is the founder of three spin out companies Warwick Effect Polymers Ltd, Medherant Ltd and Halcyon3D Ltd.

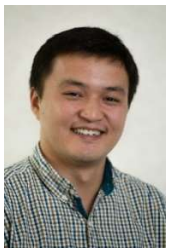

Gabit Nurumbetov obtained his PhD from the University of Warwick in 2013. In 2015 he joined Medherant Ltd after gaining extensive experience in polymer chemistry research during his PhD and post-doctoral training at the University of Warwick, contributing to over 18 publications. He oversees the research underlying the development of Medherant's novel transdermal delivery technologies and formulates TEPI Patch® products for the company and its collaborators.

Emma Pickwell-MacPherson studied natural sciences for her undergraduate degree at Cambridge University followed by an MSci in Physics where she specialized in semiconductor physics. She started her PhD with the Semiconductor Physics Group at Cambridge University and TeraView Ltd, a company specializing in terahertz imaging in 2002. Her PhD work focused on understanding contrast mechanisms in terahertz images of skin cancer.

Having completed her PhD in 2005, she worked for TeraView Ltd as a Medical Scientist until moving to Hong Kong in 2006. Prof MacPherson set up a terahertz laboratory at the Department of Electronic Engineering, CUHK during her post between 2006 and 2009 as an Assistant Professor. She spent 3 years at HKUST as a Visiting Assistant Professor (September 2009-2012) and returned to the Department of Electronic Engineering, CUHK in Sept 2012. Prof MacPherson has been on the International Organising Committee for the Infrared and Millimeter Wave and Terahertz Wave (IRMMW-THz) conference series since 2009 and she was the General Conference Chair of the 2015 IRMMW-THz conference held at CUHK. In 2017 she won a Wolfson Merit award to support her return to the UK at Warwick University, and joined the Ultrafast Photonics group in the Physics department as a Reader in October 2017. Prof MacPherson is PI of the £8M EPSRC Programme grant, "Terabotics" which is combining advances is THz technology and surgical robotics. Her research has featured on Sky news international TV (Prof. Emma MacPherson talks to Sky News International about her skin cancer research https://vimeo.com/757511937/c9a3e8cbd7) and she was promoted to Professor in 2021.

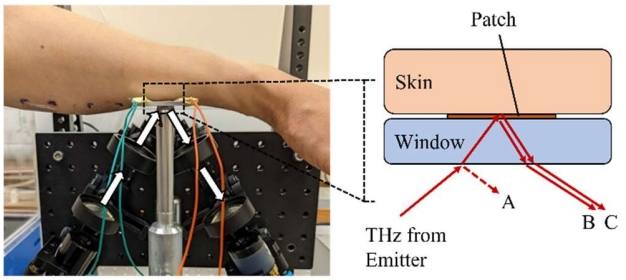

Fig. 1. A Menlo Systems Tera K15 fibre-coupled THz TDS set up in reflection geometry to measure an arm with TDD patches applied with a schematic of the highlighted region.

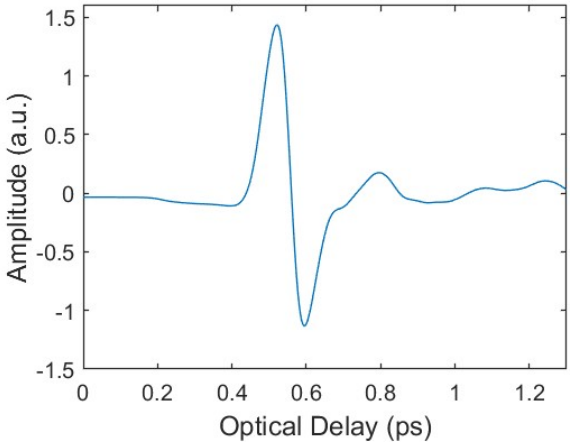

Fig. 2. An example of a THz reference signal used in the sparse deconvolution of measured THz reflected signals. This reference was obtained by measuring the reflection off a thick piece of quartz placed at the sample measuring location.

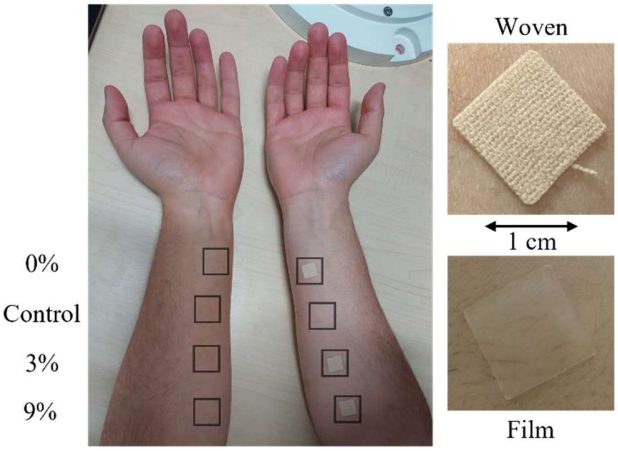

Fig. 3. A photo with boxes to highlight skin locations for where the patches and control areas typically were. Film patches are applied to the left arm and woven patches to the right arm. Close-up photos of each patch type shown to the right.

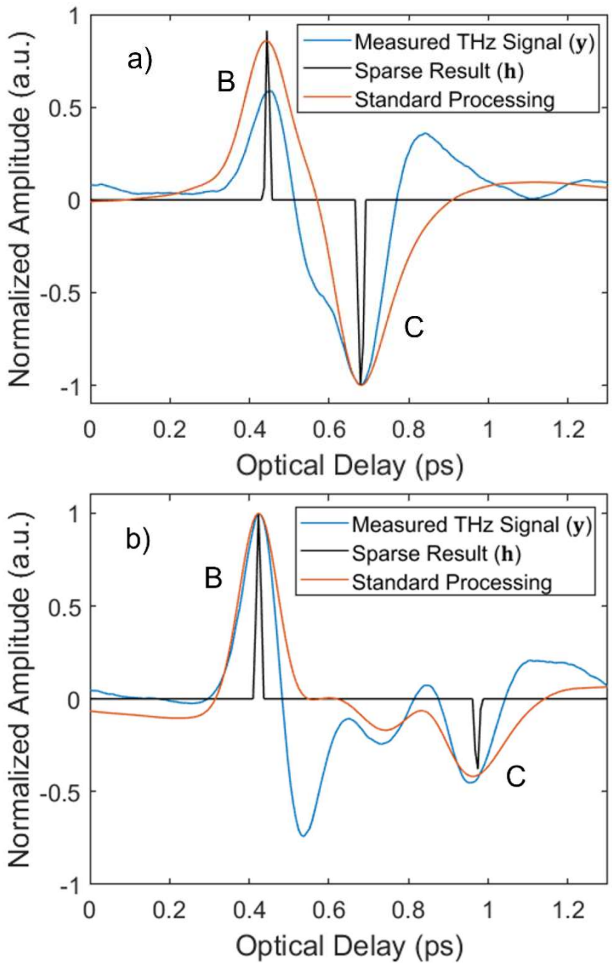

Fig. 4. The measured reflected THz signals (**y**), the deconvolution results from sparse deconvolution (**h**) and a standard THz processing method result for a) the film backed patch and b) the woven backed patch, both with 0% propylene glycol. The peak labels correspond with those schematically shown in fig. 1.

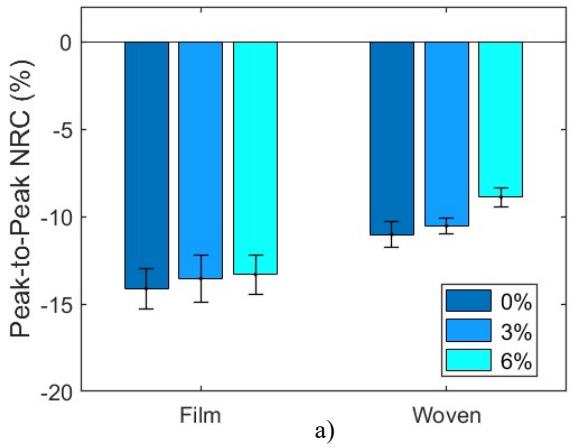

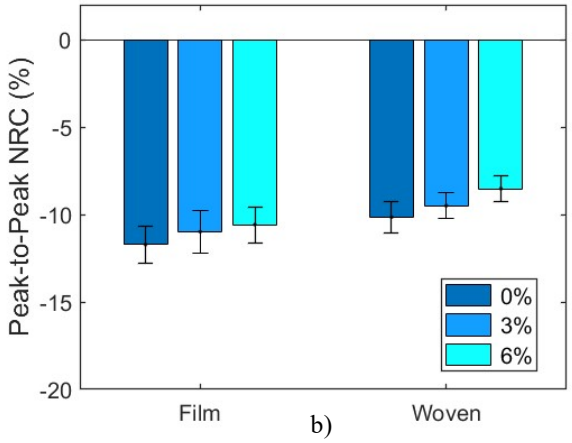

Fig. 5. The average peak-to-peak normalized relative change in skin over a 24-hour period for 14 volunteers with a) transdermal drug delivery patches applied and b) the same location but with patches removed. The color indicates differing excipient levels of 0%, 3% and 6% propylene glycol. Data for film backed patches is located on the left side of the figures, with woven backed data on the right. Error bars are the standard error on the mean.

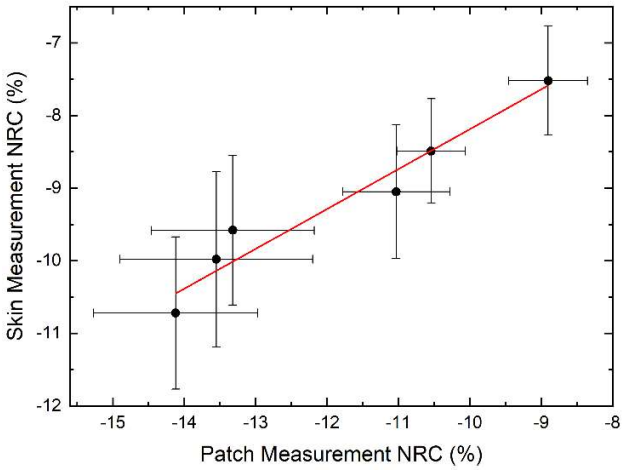

Fig. 6. A demonstration of the correlation between the NRC in measurements through the patch and of the bare skin presented in fig. 5. The red line shows the line of best fit, with a correlation coefficient of $r = 0.97$. Error bars are the standard error on the mean.

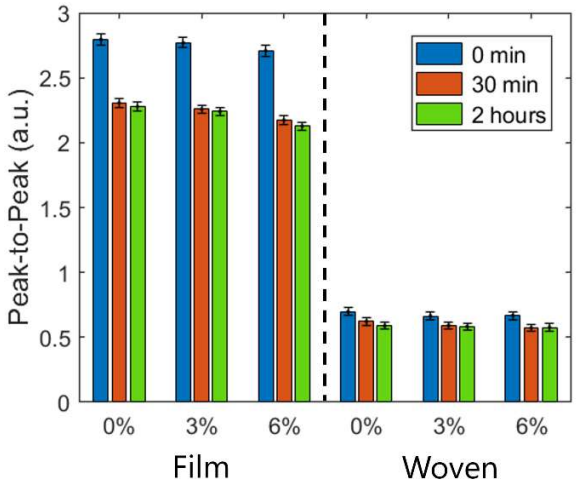

Fig. 7. The average peak-to-peak observed in 8 volunteers at 0 minutes, 30 minutes and 2 hours following the application of transdermal drug delivery patches. The patches consisted of film backed and woven backed types, with different excipient levels of 0%, 3% and 6% propylene glycol. The error bars are the standard error on the mean.